Journal of Enzyme Inhibition and Medicinal Chemistry, April 2007; 22(2): 239–246

The inhibitory effect of some new synthesized xanthates on mushroom tyrosinase activities

M. ALIJANIANZADEH[1], A. A. SABOURY[1], H. MANSURI-TORSHIZI[2], K. HAGHBEEN[3], & A. A. MOOSAVI-MOVAHEDI[1]

[1]*Institute of Biochemistry and Biophysics, University of Tehran, Tehran, Iran,* [2]*Department of Chemistry, University of Sistan & Bluchestan, Zahedan, Iran, and* [3]*The National Research Center for Genetic Engineering and Biotechnology, Tehran, Iran*

(Received 21 August 2006; in final form 23 October 2006)

Abstract

Three iso-alkyldithiocarbonates (xanthates), as sodium salts, $C_3H_7OCS_2Na$ (**I**), $C_4H_9OCS_2Na$ (**II**) and $C_5H_{11}OCS_2Na$ (**III**), were synthesized, by the reaction between CS_2 with the corresponding iso-alcohol in the presence of NaOH, and examined for inhibition of both cresolase and catecholase activities of mushroom tyrosinase (MT) from a commercial source of *Agricus bisporus*. 4-[(4-methylbenzo)azo]-1,2-benzendiol (MeBACat) and 4-[(4-methylphenyl)azo]-phenol (MePAPh) were used as synthetic substrates for the enzyme for the catecholase and cresolase reactions, respectively. Lineweaver-Burk plots showed different patterns of mixed and competitive inhibition for the three xanthates and also for cresolase and catecholase activities of MT. For cresolase activity, **I** and **II** showed a mixed inhibition pattern but **III** showed a competitive inhibition pattern. For catecholase activity, **I** showed mixed inhibition but **II** and **III** showed competitive inhibition. These new synthesized compounds are potent inhibitors of MT with K_i values of 9.8, 7.2 and 6.1 μM for cresolase inhibitory activity, and also 12.9, 21.8 and 42.2 μM for catecholase inhibitory activity for **I**, **II** and **III**, respectively. They showed a greater inhibitory potency towards the cresolase activity of MT. Both substrate and inhibitor can be bound to the enzyme with negative cooperativity between the binding sites ($\alpha > 1$) and this negative cooperativity increases with increasing length of the aliphatic tail in these compounds in both cresolase and catecholase activities. The cresolase inhibition is related to the chelating of the copper ions at the active site by a negative head group (S^-) of the anion xanthate, which leads to similar values of K_i for all three xanthates. Different K_i values for catecholase inhibition are related to different interactions of the aliphatic chains of **I**, **II** and **III** with hydrophobic pockets in the active site of the enzyme.

Keywords: *Mushroom tyrosinase, n-alkyl xanthate, mixed inhibition, competitive inhibition, inhibition constant*

Introduction

Tyrosinase (MT) (monophenol mono-oxygenase; polyphenol oxidase; catechol oxidase; and oxygen oxidoreductase; EC 1.14.18.1) is a bifunctional enzyme, which catalyzes ortho-hydroxylation of monophenols (cresolase activity) and oxidation of catechols to the corresponding ortho-quinones (catecholase activity). Tyrosinase is a copper-containing enzyme, responsible for the formation of pigment in the skin, hair, and eye [1–7]. o-Quinones follow some other enzymatic and nonenzymatic reactions, which result in formation of biopolymers like melanin [8,9]. Tyrosinases are widely distributed among animals, plants and fungi [3,10]. They are responsible for many biologically essential functions, such as pigmentation, sclerotization, primary immune response and host defense [11,12]. In mushroom (*Agaricus bisporus*), as well as in fruits and vegetables, the enzyme is responsible for browning, a commercially undesirable phenomenon [10,13,14]. Common mushroom tyrosinase (MT) from the species *Agraricus bisporus* has a molecular mass of 120 kD, is composed of two H subunits (43 kD) and two L subunits (13 kD) and contains two active sites [15,16]. Its active site has a

Correspondence: A. A. Saboury Institute of Biochemistry and Biophysics, University of Tehran, Tehran, Iran, Tel: +98-21-66956984, Fax: +98-21-66404680E-mail: saboury@ut.ac.ir

ISSN 1475-6366 print/ISSN 1475-6374 online © 2007 Informa UK Ltd.
DOI: 10.1080/14756360601114536

di-copper center, resembling that of hemocyanins [12–17] but not identical [18]. Each copper ion in the active site is coordinated by three nitrogen atoms coming from three adjacent histidine residues and the enzyme can exist in three forms; met, oxy, and deoxy [19,20]. Mettyrosinase contains two tetragonal Cu(II) ions antiferromagnetically coupled through an endogenous bridge, although hydroxide exogenous ligands other than peroxide are bound to the copper site. This species can be converted by addition of peroxide to oxytyrosinase, which in turn decays back to mettyrosinase when the peroxide is lost. Oxytyrosinase also consists of two tetragonal Cu(II) atoms, each coordinated by two strong equatorial and one weaker axial ligands. The exogenous oxygen molecule is bound as peroxide and bridges the two Cu centers. Deoxytyrosinase has a bicuprous structure (Cu(I))-Cu(I)). Structural models for their active site have been proposed [12,21,22]. In the food industry, tyrosinase is a very important enzyme in controlling the quality and economics of fruits and vegetables [23,24]. Tyrosinase is responsible for the enzymatic browning of fruits and vegetables. In addition to the undesirable color and flavor, the quinone compounds produced in the browning reaction may irreversibly react with the amino and sulfhydryl groups of proteins. The quinone-protein reaction decreases the digestibility of the protein and the bioavailability of essential amino acids, including lysine and cysteine. Therefore, development of high-performance tyrosinase inhibitors is much needed in the agricultural and food fields [25]. Tyrosinase inhibitors have attracted interest recently due to undesired browning in vegetables and fruits in post-harvest handling [26]. Additionally, tyrosinase inhibitors may be clinically used for treatment of some skin disorders associated with melanin hyper-pigmentation and are also important in cosmetics for skin whitening effects [27–30]. Also tyrosinase may play a role in neuromelanin formation in the human brain and is central to dopamine neurotoxicity as well as contribute to the neurodegeneration associated with Parkinson's disease [31]. There is a vast variety of natural and synthetic inhibitors known against catecholase, cresolase or both reactions of tyrosinase. Polyphenols, aldehydes and their derivatives are the most important inhibitors from plant natural sources [32–36]. Besides higher plants, some compounds from fungal sources have also been identified, e.g. metallothionein from *Aspergillus niger* has strong avidity to chelate copper at the active site of MT, thereby acting as a strong inhibitor [37]. Kojic acid, an antibiotic, produced by species of *Aspergillus* and *Penicillium* in the aerobic process acts as a potent, "slow-binding", competitive inhibitor of tyrosinase [38–42], and is widely used as a cosmetic whitening agent [43–45]. Synthetic tyrosinase inhibitors currently used as drugs are captopril, an antihypertensive drug, and methimazole [46,47]. Simple chemical species capable of binding to copper, such as cyanide, azide, and halide ions behave, as expected, as purely competitive inhibitors towards dioxygen binding, even if sharp differences have been seen among polyphenoloxidases from different sources [48]. Sulfur-containing compounds such as tiron, thiol and sulfites are among the most important tyrosinase inhibitors, the most commonly applied inhibitor of the discoloration process currently being sulfite [26].

To understand the mechanism of the enzyme's action and inhibition, we have attempted to obtain additional information about the structure, function and relationship of MT [49–53]. After introducing two new bi-pyridine synthetic compounds as potent uncompetitive MT inhibitors [54], the inhibitory effects of three synthetic n-alkyl dithiocarbamates, with different tails, were elucidated [55]. The binding process for catecholase inhibition by benzenethiol showed the predominance of hydrophobic interaction in the active site of the enzyme, whereas electrostatic interaction can be important for cresolase inhibition [56]. Understanding the role of hydrophobic and electrostatic interactions of inhibitor binding to the active site of the enzyme can lead to the design of new potent MT inhibitors. Hence, in the present investigation the inhibitory effects of three new synthesized alkyl xanthates, sodium salts, with different aliphatic tails, of C3, C4 and C5, are described and the kinetics of their inhibition has been elucidated for both cresolase and catecholase activities.

Materials and methods

Materials

Mushroom tyrosinase (MT; EC 1.14.18.1; specific activity 3400 units/mg) was purchased from Sigma. 4-[(4-methylbenzo)azo]-1,2-benzendiol (MeBACat) (Figure 1a) and 4-[(4-methylphenyl)azo]-phenol (MePAPh) (Figure 1b), as synthetic substrates for the enzyme for catecholase and cresolase reactions, respectively, were prepared as previously described [57].

Iso-propyl xanthate (**I**), iso-butyl xanthate (**II**) and iso-pentyl xanthate (**III**), sodium salts (Figure 1c), were synthesized. iso-Propanol, iso-butanol, iso-pentanol, carbon disulfide and sodium hydroxide were purchased from Merck Chemical Co. Germany and used as received. Infrared spectra were obtained on a Nicolet 5-DXB FT-IR spectrophotometer in the range 4000-400 cm^{-1} in KBr pellets. Microchemical analysis of carbon and hydrogen were carried out on CHN Rapid Herause. ^1H NMR spectra were recorded on a Brucker DRX-500 Avance spectrophotometer at 500 MHz in DMSO-d_6 using sodium-3-trimethylpropionate as internal reference. ^1H NMR data are expressed in part per million (ppm) and are reported as chemical shift position (δH), multiplicity (s = singlet,

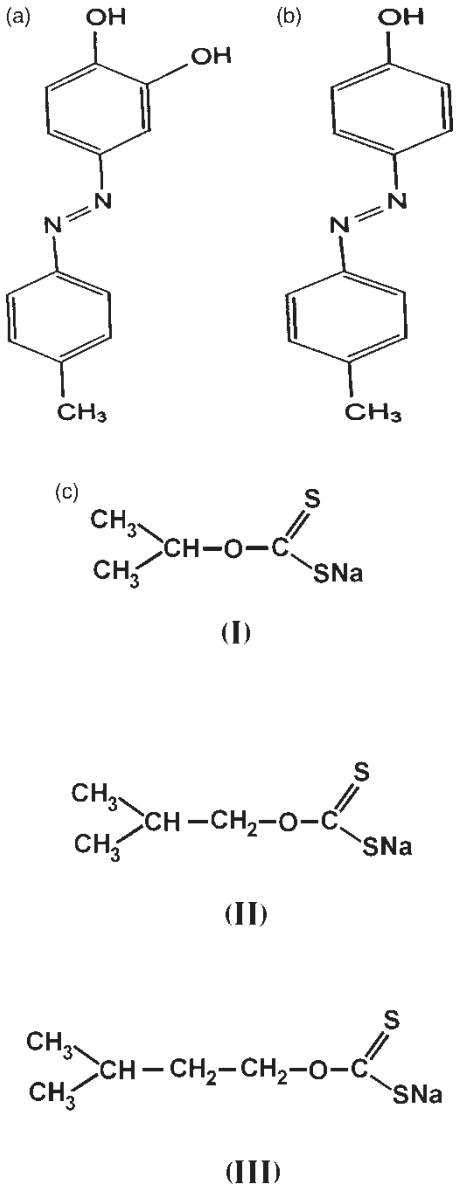

Figure 1. **(a)** 4-[(4-methylbenzo)azo]-1,2-benzendiol (MeBACat) and (b) 4-[(4-methylphenyl)azo]-phenol (MePAPh) (b), as synthetic substrates of MT for catecholase and cresolase reactions, respectively. (c) Iso-propyl xanthate (**I**), iso-butyl xanthate (**II**) and iso-pentyl xanthate (**III**), sodium salts (c) as three new MT inhibitors.

d = doublet, t = triplet, q = quartet, m = multiple) and assignment. Melting points were measured on a Unimelt capillary melting point apparatus and are reported uncorrected.

Phosphate buffer (10 mM, pH 6.8) was used throughout this work and the corresponding salts were obtained from Merck. All experiments were carried out at a temperature of 20°C.

Methods

Synthesis of sodium iso-propyl xanthate (I). This compound was prepared by an improved procedure as compared to that given in the literature [58]. 4 g (100 mmol) NaOH and 20.3 mL (100 mmol) iso-propyl alcohol were mixed together and stirred to get homogenous curdy solution. The mixture was kept in an ice bath and 20 mL of CS_2 (200 mmol) was added dropwise with constant stirring over a period of 30 min, the solution becoming cloudy yellow. Then the mouth of the reaction vessel was closed using a proper stopper and the mixture left to stir for 1 h in the ice bath and 2 h at room temperature. This crude product was completely dried at 35°C, powdered in a mortar and the powder stirred with 30 mL acetone for 15 min, and then filtered to remove undissolved particles. To the filtrate 40 mL diethylether was added and the mixture kept in the refrigerator overnight. The bright yellow crystals obtained were filtered and washed twice with ether and dried at 35°C. (yield 11.85 g, 75 mmol, 75%; decomposes at 127°C). ^{1}H NMR (500 MHz, DMSO-d_6, ppm): 5.42 (m, O-CH), 1.14 (d, O-CH$(CH_3)_2$). Analysis Calculated for $C_4H_7OS_2Na$: C, 30.38; H, 4.31. Found: C, 30.41; H, 4.26%. Solid-state IR spectroscopy of xanthates shows two characteristic bands between 1189 and 1070 cm^{-1} [58–60] assigned to $\nu_{c\text{-}o}$ and $\nu_{c\text{-}s}$ modes. Sodium iso-propyl xanthate shows similar bands at 1187 and 1035 cm^{-1}.

Synthesis of sodium iso-butyl xanthate (II). This compound was prepared by following the same procedure as described for $(CH_3)_2$CHOCSSNa except that iso-butanol 21.50 ml (100 mmol) was used instead of iso-propanol. (yield 14.79 g, 86 mmol, 86%; decomposes at 105°C). ^{1}H NMR (500 MHz, DMSO-d_6, ppm): 3.95 (m, O-CH_2), 1.88 (m, O-CH_2-CH), 0.86 (d, O-CH_2-CH$(CH_3)_2$). Analysis Calculated for $C_5H_9OS_2Na$: C, 34.88; H, 5.23. Found: C, 34.52; H, 5.12%. Solid-state IR spectroscopy of showed bands at 1158 and 1076 cm^{-1}.

Synthesis of sodium iso-pentyl xanthate (III). This compound was prepared by following the same procedure as described for $(CH_3)_2$CHOCSSNa except that iso-pentanol (22.68 ml, 100 mmol) was used instead of iso-propanol (yield 15.63 g, 84 mmol, 84%; decomposes at 88°C). ^{1}H NMR (500 MHz, DMSO-d_6, ppm): 4.20 (t, O-CH_2), 1.46 (m, O-CH_2-CH_2), 1.63 (m, O-CH_2-CH_2-CH), 0.86 (d, O-CH_2-CH_2-CH$(CH_3)_2$). Analysis Calculated for $C_6H_{11}OS_2Na$: C, 38.71; H, 5.1. Found: C, 38.82; H, 5.2%. Solid state IR spectroscopy showed two characteristic bands at 1158 and 1074 cm^{-1}.

Kinetic measurements. Kinetic assay of catecholase and cresolase activities was carried out through depletion of MeBACat and MePAPh, respectively, for 1 and 2

min, with enzyme concentrations of 11.11 and 112.68 μg/mL, at wavelengths of 473 nm and 352 nm using a Cary spectrophotometer, 100 Bio-model, with jacketed cell holders. Freshly prepared enzyme, substrate, **I**, **II**, and **III** were used in this work. All enzymatic reactions were run in phosphate buffer (10 mM) at pH 6.8 in a conventional quartz cell, thermostated to maintain the temperature at 20 ± 0.1°C. Substrate addition followed after incubation of enzyme with different concentrations of the n-alkyl xanthate.

Results and discussion

The inhibitory effects of three different ligands on both MT activities were examined at pH 6.8 and a temperature of 20°C.

Kinetic parameters of cresolase activity of MT in the presence of I, II and III:

Double reciprocal Lineweaver-Burk plots for the cresolase activity of MT on hydroxylation of MePAPh, as the substrate, in the presence of different fixed concentrations of **I**, **II** and **III** are shown in Figures 2a, 3a and 4, respectively. These plots show a set of straight lines, which intersect on the left hand side of the vertical axis, close to the horizontal axis for **I** (see Figure 2a) and a little further from the horizontal axis for **II** (Figure 3a), which confirms mixed inhibition. The apparent maximum velocity (V_{max}') and apparent Michaelis constant (K_m') values as well as the slope values of these straight lines (K_m'/V_{max}') can be obtained at different fixed concentrations of each inhibitors (**I** and **II**). A secondary plot of the slope against the concentration of inhibitor gives a straight line with an abscissa-intercept of $-K_i$ (see Figures 2b and 3b for **I** and **II**, respectively) and also another secondary plot of the reciprocal apparent maximum velocity against the concentration of inhibitor gives a straight line with an abscissa-intercept of $-\alpha K_i$ (see Figures 2c and 3c for **I** and **II**, respectively), where K_i is the inhibition constant and α is the interaction factor between the substrate and inhibitor sites. Double reciprocal Lineweaver-Burk plot for **III** gives a set of straight lines intersecting exactly on the vertical axis, the value of the maximum velocity (V_{max}) is unchanged by the inhibitor but the K_m' value is increased, confirming competitive inhibition for **III** (see Figure 4). The inset on Figure 4 shows the secondary plot of the K_m' at any concentration of inhibitor (**III**) versus the concentration of inhibitor, which gives the inhibition constant ($-K_i$) from the abscissa-intercepts.

Results for K_i and α values for the cresolase activity of MT in the presence of **I**, **II** and **III** have been summarized in Table I. The α value for **I** is 1.2. An α value equal to one means that the mode of inhibition is

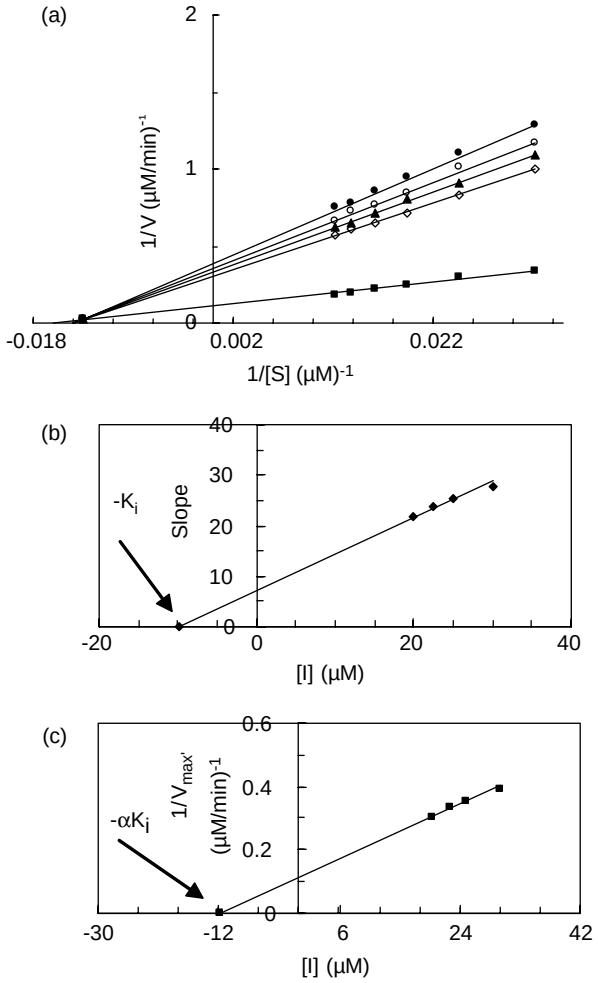

Figure 2. (a) Double reciprocal Lineweaver-Burk plots of MT kinetics assays for cresolase reactions of MePAPh in 10 mM phosphate buffer, pH 6.8, at temperature of 20°C and 112.68 μg/mL enzyme concentration, in the presence of different concentrations of **I**: 0 mM (■), 0.02 mM (◇), 0.0225 mM (▲), 0.025 mM (○), 0.03 mM (●). (b) Secondary plot of the slope against the concentration of inhibitor, which gives the $-K_i$ from the abscissa-intercept. (c) Secondary plot of $1/V_{max}'$ versus concentration of inhibitor, which gives $-\alpha K_i$ from the abscissa-intercept.

noncompetitive. In noncompetitive inhibition there is no interaction between substrate and inhibitor binding sites. Hence, there is a weak interaction, negative cooperativity, between substrate and **I** binding sites causing some deviation for α value from one (i.e. it is equal to 1.2). The α value for **II** is 4.1 which means that the negative cooperativity between substrate and inhibitor has been increased due to the addition of a $-CH_2-$ group to the molecular structure of the ligand. Addition of a further $-CH_2-$ group has led to competitive inhibition for **III** with an infinite value for α which means that the interaction between substrate and inhibitor binding sites is so high that only substrate or inhibitor can bind to the enzyme. As shown in Table I, the largest value of K_i is for **I**

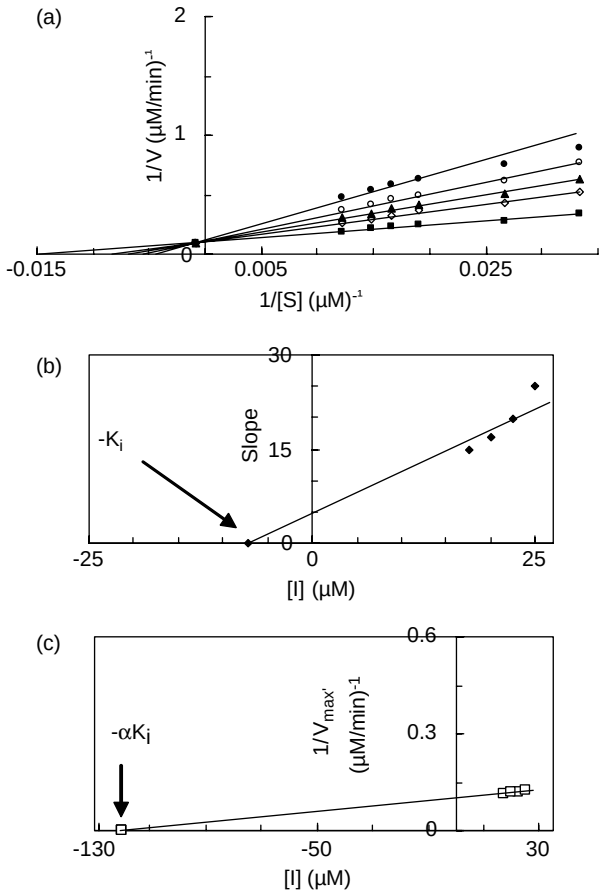

Figure 3. (a) Double reciprocal Lineweaver-Burk plots of MT kinetic assay for cresolase reactions of MePAPh in 10 mM phosphate buffer, pH 6.8, at temperature of 20°C and 112.68 μg/mL enzyme concentration, in the presence of different concentrations of **II**: 0 mM (■), 0.0175 mM (◇), 0.02 mM (▲), 0.0225 mM (○), 0.025 mM (●). (b) Secondary plot of the slope against the concentration of inhibitor, which gives the $-K_i$ from the abscissa-intercept. (c) Secondary plot of $1/V_{max}'$ versus concentration of inhibitor, which gives $-\alpha K_i$ from the abscissa-intercept.

(9.8 μM) and the smallest is for **III** (6.1 μM). So the affinity of inhibitor binding to the enzyme does not change largely from **I** to **III**; it changes slightly in the order of **I** < **II** < **III**. Although extending the size of the inhibitor molecule by adding a $-CH_2-$ group causes more negative cooperativity in the binding sites of substrate and inhibitor, the affinity of binding is slightly increased.

Kinetic parameters of catecholase activity of MT in the presence of I, II and III

Double reciprocal Lineweaver-Burk plots for the catecholase activity of MT on oxidation of MeBACat as substrate, in the presence of different fixed concentrations of **I**, **II** and **III** at pH 6.8 and temperature 20°C are shown in Figures 5a, 6 and 7, respectively. This plot for **I** gives a set of straight lines, which intersect on the left hand side of the vertical

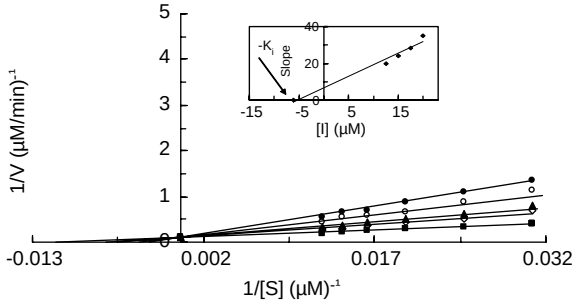

Figure 4. Double reciprocal Lineweaver-Burk plots of MT kinetic assay for cresolase reactions of MePAPh in 10 mM phosphate buffer, pH 6.8, at temperature of 20°C and 112.68 μg/mL enzyme concentration, in the presence of different concentrations of **III**: 0 mM (■), 0.0125 mM (◇), 0.015 mM (▲), 0.0175 mM (○), 0.02 mM (●). Inset: secondary plot of the slope against different concentrations of inhibitor, which gives the inhibition constant ($-K_i$) from the abscissa-intercept.

axis, close to the horizontal axis (see Figure 5a), which confirms mixed inhibition. Secondary plots of the slope against the concentration of inhibitor and the reciprocal of apparent maximum velocity against the concentration of inhibitor give straight lines with abscissa-intercepts of $-K_i$ (see Figure 5b) and $-\alpha K_i$ (see Figure 5c), respectively. Double reciprocal Lineweaver-Burk plots for **II** and **III** give a set of straight lines intersecting exactly on the vertical axis, confirming competitive inhibition (see Figures 6 and 7 for **II** and **III,** respectively). The insets on Figures 6 and 7 show the secondary plots, which give the inhibition constants ($-K_i$) from the abscissa-intercepts.

Results for K_i and α-values of catecholase activity of MT in the presence of **I, II** and **III** have been summarized in Table I. The α-value for **I** is 2 which means that there is negative cooperativity between substrate and inhibitor binding sites but this interaction is not very strong. Infinite α-values for **II** and **III** mean that by adding one or two $-CH_2-$ groups to the molecular structure of ligand the interaction between substrate and inhibitor binding sites becomes so high that only substrate or inhibitor can bind to the enzyme. As shown in Table I, the greatest value of K_i is for **III** (42.2 μM) and the smallest for **I** (12.9 μM). The affinity of inhibitor binding to the enzyme is in the order **III** < **II** < **I.** Although extending the size of the inhibitor molecule by adding a $-CH_2-$group causes more negative cooperativity in the binding sites of substrate and inhibitor, the affinity of binding is decreased.

The change of the standard Gibbs free energy of binding (ΔG°) for each inhibitor was calculated using the association binding constant (K_a), obtained from the inverse of the K_i value, in the equation $\Delta G^\circ = -RT \ln K_a$; where R is the gas constant and T is the absolute temperature [61]. The calculated ΔG° values of the three ligands for cresolase and catecholase

Table I. Thermodynamic parameters of binding 2-Propanol dithioxantate (**I**), iso-butanol dithioxantate (**II**) and iso-pentanol dithioxantate (**III**), sodium salts, on mushroom tyrosinase at temperature 20°C and pH 6.8.

Reaction type	Ligands	K_a $(M)^{-1}$	K_i (μM)	$\Delta G°(kJ\ mol)^{-1}$	α
Catecholase activity	**I**	7.8×10^4	12.9	−27.4	2.0
	II	4.6×10^4	21.8	−26.1	∞
	III	2.3×10^4	42.2	−24.6	∞
Cresolase activity	**I**	1.0×10^5	9.8	−28.1	1.2
	II	1.4×10^5	7.2	−28.9	4.1
	III	1.6×10^5	6.1	−29.2	∞

K_a: association constant, K_i: inhibition constant; α: interaction factor

activities are summarized in Table I. The inhibitor binding process is spontaneous ($\Delta\mathring{G} < 0$) in all cases, although for cresolase inhibition the binding process occurs more favorably.

Some thiol compounds acts as inhibitors of tyrosinase due to their ability to chelate Cu^{+2} [62]. All of our new synthesized compounds also act as inhibitors. Each n-alkyl xanthate (sodium salt) produces an anion with a head S^-group and a hydrophobic tail. The comparison of K_i and $\Delta G°$ values in Table I reveals that these three ligands have inhibited the cresolase activity more strongly than the catecholase activity of MT. As reported previously [56], here our results also show that the type of inhibitor binding process is different in the two types of MT activities. The predominant interaction in the active site of the enzyme for the binding process of catecholase inhibition is hydrophobic, whereas the electrostatic interaction can be important for cresolase inhibition [56]. Hence, we expect all three xanthates to have approximately identical K_i values for cresolase activity due to the same charged head group. However, different values of K_i for catecholase activity are expected due to different tails for these three xanthates. Moreover, K_i values increase in magnitude as the length of the hydrophobic tail increases for these compounds, which means that a shorter tail gives a more potent inhibitor. This result is the same as our previous result [55]. Hydrophobic interaction between the tail of the ligand and hydrophobic pockets in the active site of the enzyme reduces the affinity of inhibitor binding in the catecholase inhibition. The cresolase activity occurs when enzyme is in the oxy-form and the catecholase activity occurs

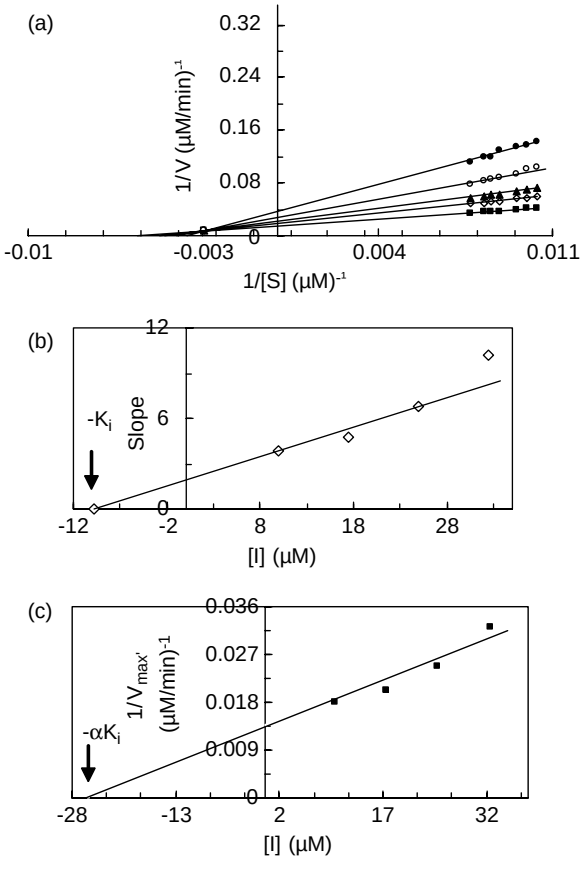

Figure 5. (a) Double reciprocal Lineweaver-Burk plots of MT kinetic assay for catecholase reactions of MeBACat in 10 mM phosphate buffer, pH 6.8, at temperature of 20°C and 11.11 μg/mL enzyme concentration, in the presence of different concentrations of **I**: O mM (■), 0.01 mM (◇), 0.0175 mM (▲), 0.025 mM (○), 0.0325 mM (●). (b) Secondary plot of the slope against the concentration of inhibitor, which gives the $-K_i$ from the abscissa-intercept. (c) Secondary plot of $1/V_{max}'$ versus concentration of inhibitor, which gives $-\alpha K_i$ from the abscissa-intercept.

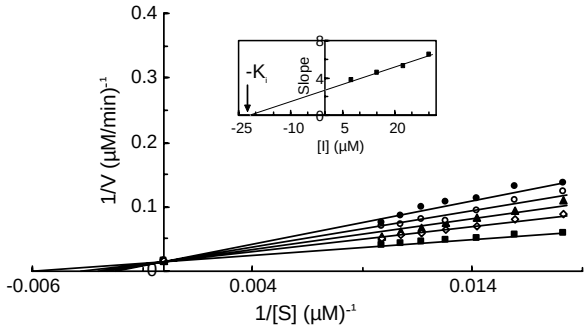

Figure 6. Double reciprocal Lineweaver-Burk plots of MT kinetic assay for catecholase reactions of MeBACat in 10 mM phosphate buffer, pH 6.8, at temperature of 20°C and 11.11 μg/mL enzyme concentration, in the presence of different concentrations of **II**: 0 mM (■), 0.0075 mM (◇), 0.015 mM (▲), 0.0225 mM (○), 0.03 mM (●). Inset: secondary plot of the slope against different concentrations of inhibitor, which gives the inhibition constant ($-K_i$) from the abscissa-intercept.

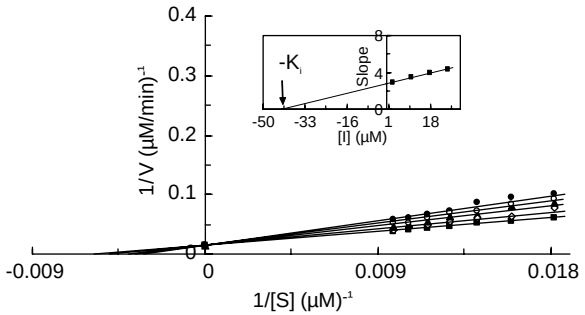

Figure 7. Double reciprocal Lineweaver-Burk plots of MT kinetic assay for catecholase reactions of MeBACat in 10 mM phosphate buffer, pH 6.8, at temperature of 20°C and 11.11 μg/mL enzyme concentration, in the presence of different concentrations of **III**: 0 mM (■), 0.0025 mM (◇), 0.01 mM (▲), 0.0175 mM (○), 0.025 mM (●). Inset: secondary plot of the slope against different concentrations of inhibitor, which gives the inhibition constant ($-K_i$) from the abscissa-intercept.

when the enzyme is in the met-form, so maybe the set of hydrophobic pockets in the oxy-form are different from these in the met-form. The structure of hydrophobic pockets of the enzyme is energetically favorable for inhibitor binding with a shorter hydrophobic chain in the catecholase activity. Our results here may assist future aims in the design of inhibitors to prevent undesirable fruit browning in vegetables or as color skin modulators in mammals.

Acknowledgements

The financial support given by the University of Tehran and the Iran National Science Foundation (INSF) are gratefully acknowledged.

References

[1] Mason HS. Mechanism of oxygen metabolism. In: Nord FF, editor. Adv Enzymol., Vol. 19 NewYork: Academic Press; 1957. p 79–233.
[2] Seo Sy, Sharma VK, Sharma N. Mushroom tyrosinase: Recent prospects. J Agric Food Chem 2003;51:2837–2853.
[3] Van Gelder CWG, Flurkey WH, Wichers HJ. Sequence and structural features of plant and fungal tyrosinases. Phytochemistry 1997;45:1309–1323.
[4] Winder AJ, Harris H. New assays for tyrosine hydroxylase and dopa oxidase activities of tyrosinase. Eur J Biochem 1991;198:317–326.
[5] Robb DA. Copper proteins and copper enzymes. Boca Raton: CRC Press; 1984.
[6] Riley PA. Tyrosinase kinetics: A semi-quantitative model of the mechanism of oxidation of monohydric and dihydric phenolic substrates. J Theor Biol 2000;203:1–12.
[7] Fenoll LG, Rodriguez-Lopez JN, Garcia-Sevilla F, Tudela J, Garcia-Ruiz PA, Varon R, et al. Oxidation by mushroom tyrosinase of monophenols generating slightly unstable oquinones. Eur J Biochem 2000;267:5865–5878.
[8] Yasunobu KT, Gordon M, editors. Pigment Cell Biology. New York: Academic Press; 1959. p 583.
[9] Raper HS. The anaerobic oxidases. Physiol Rev 1928;8: 245–282.
[10] Whitaker JR In: Wong DWS, editor. Food enzymes, structure and mechanisms. New York: Chapman and Hall; 1995. p 271–307.
[11] Jaenicke E, Decker H. Tyrosinases from crustaceans form hexamers. Biochem J 2003;371:515–523.
[12] Sanchez-Ferrer A, Rodriguez-Lopez JN, Garcia-Canovas F, Garcia-Carmona F. Tyrosinase: A comprehensive review of its mechanism. Biochim Biophys Acta 1995;1247:1–11.
[13] Xie LP, Chen QX, Huang H, Wang HZ, Zhang RQ. Inhibitory effects of some flavonoids on the activity of mushroom tyrosinase. Biochemistry (Mosc) 2003;68:487–491.
[14] Martinez MV, Whitaker JR. The biochemistry and control of enzymatic browning. Trends Food Sci Technol 1995;6: 195–200.
[15] Strothkemp KJ, Jolley RL, Mason Hs. Quaternary structure of mushroom tyrosinase. Biochem Biophys Res Commun 1976;70:519–524.
[16] Yong G, Leone C, Strothkemp KJ. Agricus bisporus metapo tyrosinase: Preparation characterization, and conversion to mixed-metal derivatives of the binuclear site. Biochemistry 1990;29:9684–9690.
[17] Orlow SJ, Bao-Kang Z, Chakraborty AK, Dricker M, Pifko-Hirst S, Pawelek JM, et al. High-molecular weight forms of tyrosinase and the tyrosinase-related proteins: Evidence for a melanogenic complex. J Invest Dermatol 1994;103:196–201.
[18] Eicken C, Krebs B, Sacchettini JC. Catechol oxidase-structure and activity. Curr Opin Struct Biol 1999;9:677–683.
[19] Cooksey CJ, Garratt PJ, Land EJ, Ramsden CA, Riley PA. Tyrosinase kinetics: Failure of the auto-activation mechanism of monohydric phenol oxidation by rapid formation of a quinomethane intermediate. Biochem J 1998;333:685–691.
[20] Rescigno A, Sollai F, Pisu B, Rinaldi A, Sanjust E. Tyrosinase inhibition: General and applied aspects. J Enz Inhib Med Chem 2002;17:207–218.
[21] Himmelwright RS, Eichman NC, Lu Bien CD, Lwrch K, Solomon EIJ. Am Chem Soc 1980;102:7339.
[22] Solomon, EI, Sundaram, UM, Machonkin, TE. Multicopper Oxidases and Oxygenases. Chem Rev 1996;96:2563–2606.
[23] Mayer AM. Polyphenol oxidases in plants: Recent progress. Phytochem 1987;26:11–20.
[24] Friedman M. Food browning and its prevention: An overview. J Agric Food Chem 1996;44:631–653.
[25] Kim YJ, Uyama H. Tyrosinase inhibitors from natural and synthetic sources: Structure, inhibition mechanism and perspective for the future. Cell Mole Life Sci 2005;62: 1707–1723.
[26] Taylor SL, Bush RK. Sulfites as food ingredients. Food Technol 1986;40:47–52.
[27] Ohyama Y, Mishima Y. Melanogenesis inhibitory effects of kojic acid and its action mechanism. Fragrance J 1990;6:53.
[28] Palumbo A, d'Ischia M, Misuraca G, Parota G. Mechanism of inhibition of melanogenesis by hydroquinone. Biochim Biophys Acta 1991;1073:85–90.
[29] Maeda K, Fukuda M. In vitro effectiveness of several whitening cosmetic components in human melanocytes. J Soc Cosmet Chem 1991;42:361–368.
[30] Mosher DB, Pathak MA, Fitzpatric TB, editors. Update: Dermatology in general medicine. New York: McGraw Hill; 1983. p 205–225.
[31] Nihei kI, Yamagiwa Y, Kamikawa T, Kubo I. 2-Hydroxy-4-isopropylebenzaldehyde, a potent partial tyrosinase inhibitor. Bioorgan Med chem Lett 2004;14:681–683.
[32] Kubo I, Kinst-Hori I. Flavonols from saffron flower: Tyrosinase inhibitory activity and inhibition mechanism. J Agric Food Chem 1999;47:4121–4125.
[33] Kubo I, Kinst-Hori I, Ishiguro K, Chaudhuri SK, Sanchez Y, Ogura T. Tyrosinase inhibitory flavonoids from heterotheca inuloides and their structural functions. Bioorg Med Chem Lett 1994;4:1443–1446.

[34] Chen QX, Kubo I. Kinetics of mushroom tyrosinase inhibition by querctin. J Agric Food Chem 2002;50:4108–4112.
[35] Kubo I, Kinst-Hori I, Chaudhuri SK, Kubo Y, Sanchez Y, Ogura T. Flavonols from heterothesca inuloides: Tyrosinase inhibitory activity and structural criteria. Bioorg Med Chem 2000;8:1749–1755.
[36] Kubo I, Kinst-Hori I. Tyrosinase inhibitors from cumin. J Agric Food Chem 1988;46:5338–5341.
[37] Goetghebeur M, Kermasha S. Inhibition of polyphenol oxidase by copper-metallothionein from aspergillus niger. Phytochemistry 1996;42:935–940.
[38] Kim YM, Yun J, Lee CK, Lee H, Min KR, Kim Y. Oxyresveratrol and hydroxystilbene compounds: Inhibitory effect on tyrosinase and mechanism of action. J Biol Chem 2002;227:16340–16344.
[39] Chen JS, Wei C, Rolle RS, Otwell WS, Balban MO, Marshall MR. Inhibitory effect of kojic acid on some plant and crustacean polyphenol oxidases. J Agric Food Chem 1991;39:1396–1401.
[40] Chen JS, Wei C, Marshall MR. Inhibition mechanism of kojic acid on polyphenol oxidase. J Agric Chem 1991;39: 1897–1901.
[41] Kahn V In: Lee CY, Whitaker JR, editors. Enzymatic browning and its prevention. Washington DC: American Chemical Society; 1995. p 277–294.
[42] Kahn V, Ben-Shalom N, Zakin V. Effect of kojic acid on the oxidation of N-acetyldopamine by mushroom tyrosinase. J Agric Food Chem 1997;45:4460–4465.
[43] Cabanes J, Chazarra S, Garcia-Carmona F. Kojic acid, a cosmetic skin agent, is a slow-binding inhibitor of catecholase activity of tyrosinase. J Pharm Pharmacol 1994;46:982–985.
[44] Lim JT. Treatment of melasma using kojic acid in a gel containing hydroquinone and glycolic acid. Dermatol Surg 1999;25:282–284.
[45] Battaini G, Monzani E, Casella L, Santagostini L, Pagliarin R. Inhibition of the catecholase activity of biomimetic dinuclear copper complexes by kojic acid. J Biol Inorg Chem 2000;5: 262–268.
[46] Espin JC, Wichers HG. Effect of captopril on mushroom tyrosinase activity in vivo. Biochim Biophys Acta 2001;1554: 289–300.
[47] Andrawis A, Khan V. Effect of methimazole on the activity of mushroom tyrosinase. Biochem J 1996;235:91–96.
[48] Ferrar PH, Walker JRI. Inhibition of diphenoloxidases: A comparative study. J Food Biochem 1996;20:15–30.
[49] Haghbeen K, Saboury AA, Karbassi F. Substrate share in the suicide inactivation of mushroom tyrosinase. Biochim Biophys Acta 2004;1675:139–146.
[50] Karbassi F, Haghbeen K, Saboury AA, Ranjbar B, Moosavi-Movahedi AA. Activity, structural and stability changes of mushroom tyrosinase by sodium dodecyl sulfate. Colloids and Surface B: Biointerfaces 2003;32:137–143.
[51] Shareefi Borojerdi S, Haghbeen K, Karkhane AA, Fazli M, Saboury AA. Successful resonance Raman study of cresolase activity of mushroom tyrosinase. Biochem Biophys Res Commun 2004;314:925–930.
[52] Gheibi N, Saboury AA, Haghbeen K, Moosavi-Movahedi AA. Activity and structural changes of mushroom tyrosinase induced by n-alkyl sulfates. Colloids and Surface B: Biointerfaces 2005;45:104–107.
[53] Karbassi F, Haghbeen K, Saboury AA, Ranjbar B, Moosavi-Movahedi AA, Farzami B. Stability, structural and suicide inactivation changes of mushroom tyrosinase after acetylation by N-acetylimidazole. Int J Biol Macromol 2004;34:257–262.
[54] Karbassi F, Saboury AA, Hassan Khan MT, Iqbal Choudhary M, Saifi ZS. Mushroom tyrosinase inhibition by two potent uncompetitive inhibitors. J Enz Inhib Med Chem 2004;19:349–353.
[55] Gheibi N, Saboury AA, Mansury-Torshizy H, Haghbeen K, Moosavi-Movahedi AA. The inhibition effect of some n-alkyl dithiocarbamates on mushroom tyrosinase. J Enz Inhib Med Chem 2004;20:393–399.
[56] Saboury AA, Zolghadri S, Haghbeen K, Moosavi-Movahedi AA. The inhibitory effect of benzenethiol on the cresolase and catecholase activities of mushroom tyrosinase. J Enz Inhib Med Chem 2006;21:in press.
[57] Haghbeen K, Tan EW. Facile synthesis of catechol azo dyes. J Org Chem 1998;63:4503–4505.
[58] Ahmed AM, Ibrahim K, Anna OR, John PF, Jr. Synthesis, characterization and luminescent properties of dinuclear Gold(I) xanthate complexes: X-ray structure of [Au_2(n-Bu-xanthate)$_2$]. Inorg Chem 2004;43:3833–3839.
[59] Fackler JP, Jr, William CS. Sulfur ligand complexes. IX. Reactions of metal xanthates and their derivatives. The formation of biophosphine-dithiocarbonate and -trithiocarbonate complexes of palladium (II) and platinum (II). Inorg Chem 1969;8:1631–1639.
[60] Katsoulos GA, Tsipis CA. Synthesis of some novel Pt (II) and Pd (II) n-alkyliminodithocarbonato complexes and investigation of the mechanism of their formation by CNDO/2 quantum chemical calculations. Inorg Chim Acta 1984;84: 89–94.
[61] Atkins P, DePaula J. Physical chemistry. 7th Ed New York: WH Freeman & Company; 2002. Chap 9 .
[62] Hanlon DP, Shuman S. Copper ion binding and enzyme inhibitory properties of the antithyroid drug methimazole. Experientia 1975;31:1005–1006.